A-PoRM SIPLAS: Assessing The Post-Disaster Recovery Of Mangrove Forest In Siargao Island Protected Landscape And Seascape (SIPLAS) Area Using Sentinel-1 SAR Data

Jay Melvin Segales [1], Eliazar Mark Paz[1], Arturo G. Cauba Jr.[1]

[1] Department of Geodetic Engineering, College of Engineering and Geosciences, Caraga Center for Geo-Informatics
Caraga State University, Ampayon, Butuan City, 8600
jaymelvin.segales@carsu.edu.ph
eliazarmark.paz@carsu.edu.ph
agcauba@carsu.edu.ph

Keywords: Sentinel-1, SIPLAS, Mangroves, Unsupervised Change Detection Method, GEE, Cumulative Sum (CuSum)

Abstract

Tropical cyclones and typhoons pose significant threats to coastal ecosystems, particularly mangrove forests. Assessing the extent of mangrove damage and monitoring recovery post-disaster is vital for effective conservation and management strategies. Space-based observations have become increasingly common in monitoring forest damage in tropical regions. However, the predominant methods for change detection rely on satellite optical imagery, which faces challenges in humid tropical zones. Technological advancements have led to the development of detection techniques utilizing synthetic aperture radar (SAR) to address cloud cover issues. The study specifically targets Siargao Island Protected Landscape and Seascape (SIPLAS), the largest contiguous forest in the Philippines, from destruction caused by Super typhoon Rai (Odette). The study utilized SAR time-series data, unsupervised log ratio change detection method and Cumulative Sum (CuSum) analysis via Google Earth Engine (GEE). Analysis of Sentinel-1 GRD images found VV polarization had the highest accuracy at 92% and an F-measure of 0.92. VH polarization had 87.5% accuracy and an F-measure of 0.87, while combining VV and VH and VV/VH achieved the same results of 80.5% overall accuracy with an F-measure of 0.82. With that, results indicated that 53% of mangroves in SIPLAS area were damaged, with 38.05% regenerating by 2022 and 56.75% by 2023, notably after September 16, 2022 detected from CuSum analysis using the VV polarization. These findings substantiate the robustness of the data and methodologies employed in monitoring mangrove resilience and supporting conservation initiatives within the SIPLAS area.

1. Introduction

The Siargao Islands, under Proclamation No. 902, was designated a protected area known as SIPLAS (Siargao Island Protected Landscape and Seascape), boasting the title as the largest marine-protected area in the Philippines (Siargao Island Protected Landscape and Seascape [SIPLAS], 2013). Its rich biodiversity and the ecological benefits of mangrove forest covers one of the largest contiguous mangrove reserves in the country (Villamente, 2023)

Mangroves are extremely important to the coastal ecosystems they inhabit. Physically, they serve as a buffer between marine and terrestrial communities and protect shorelines from damaging winds, waves, and floods. Mangrove thickets improve water quality by filtering pollutants and trapping sediments from the land, and they reduce coastal erosion. Ecologically, mangroves provide habitat for diverse terrestrial organisms and serve as breeding, spawning, and hatching grounds for numerous coastal species (Encyclopedia Britannica, 2019). A comprehensive news report by the Nature Conservancy (2021) shows that mangroves are one of the world’s most important ecosystems. Healthy mangrove forests are hotspots of biodiversity, foundations of climate resilience and a source of livelihoods for coastal communities worldwide. They are carbon stores, fish factories, coastal defenses and more, conveying incalculable benefits to both people and planet.

The Department of Environment and Natural Resources (DENR) defines mangroves as a part of the coastal and marine ecosystem that includes seagrass and coral reefs. Out of the world’s more than 70 salt-tolerant mangrove species, around 46 species exist in the Philippines. The mangrove is known as the “rainforest of the sea” and like the inland rainforest, a mangrove provides both economic and ecological benefits to the coastlines. Mangroves are a source of alcohol, medicines, tannin, timber, and housing materials (Viray-Mendoza, 2017). Moreover, mangroves provide an effective natural buffer against storms, flooding, coastal erosion, and strong waves (Stringer and Orchard, 2013).

However, the Philippines is particularly susceptible to typhoons due to its geographical location, experiencing an average of 20 typhoons annually, each varying in intensity. These typhoons bring heavy rainfall, strong winds, storm surges, and flooding, causing significant damage to infrastructure, agriculture, and the economy (Santos, 2021). Recently, the Philippines experienced a super typhoon Rai, locally known as Odette, made landfall over five Philippine regions last Dec. 16, 2021, causing widespread destruction and fatalities to human and environment. One of the most affected areas of typhoon Odette was the Siargao islands, situated at the northeastern part of Mindanao (NASA Applied Sciences, 2021).

Undeniably, Siargao Islands, home to the largest mangrove forest in the Philippines, particularly in the municipality of Del Carmen, covering 4,871 hectares as of 2018, was severely impacted by typhoon Odette. This mangrove forest is the habitat of rare and endangered species of flora and fauna both in marine, wetland, and terrestrial areas. This ecosystem helps maintain the island's ecological balance by providing rich breeding grounds for aquatic lives. Furthermore, the forest plays an important role in capturing and storing carbon and helps the Philippines to meet its goal of carbon emission reduction. In addition to creating habitats and storing carbon, the forest also protects the community from the inevitable effects of climate change disasters (Urban Nature Atlas, 2022). In December 2021, it was able to protect the residents from the onslaught of Typhoon Odette, however due to the extremities brought by the typhoon, most of the mangrove forests were disrupted (One News PH, 2017). Typhoon Odette ravaged agriculture, infrastructure, and environment on the island and damaged the plantation of mangroves. Mangrove forest were among those severely damaged in Surigao del Norte and from now on, matured mangrove species in Barangay Mabuhay, Del Carmen, are still down (Philippine News Agency, 2022).

As defined by NASA (2020), Synthetic Aperture Radar, or SAR, is an active remote sensing approach that sends out a signal with known wavelength and measures backscatter. Compared to a passive system that receives thermal emissions or reflected components, SAR allows for penetration through most clouds and precipitation, varying with wavelength (Molthan et al., 2017) . Since it can penetrate cloud cover and “see through” darkness and weather, it will allow a unique view of flood inundation, land cover changes, and modifications of the Earth's surface from landslides, earthquakes, and background tectonic motion (Earth Science Data Systems, 2024).

In response to this occurrence, this study focused on conducting a post-disaster assessment of mangrove biodiversity, particularly in the SIPLAS area, to understand the extent of damage, trend and recovery patterns. The researchers utilized Synthetic Aperture Radar (SAR) data to assess the recovery of mangrove biodiversity in the specified region of study. Through this study, the researchers can primarily improve the understanding of post-disaster mangrove recovery processes, inform conservation and restoration efforts, and contribute to the sustainable management of mangrove ecosystems in SIPLAS area.

1.1 Study Area

This study focused on Siargao Island Protected Landscape and Seascape (SIPLAS) (Figure 1), a protected area located in Surigao del Norte, Philippines, with central coordinates around 9.8833° N latitude and 126.0333° E longitude (The Philippines Today, 2021). SIPLAS encompasses a comprehensive geographical scope, spanning nine (9) municipalities and comprising 48 barangays (Visit Del Carmen, 2018). The protected area covers a substantial land area of around 280 square kilometers, encompassing both terrestrial and marine ecosystems. SIPLAS is notable for hosting the largest contiguous mangrove forest in the country, spanning approximately 9,000 hectares. The island experienced significant devastation from Typhoon Rai (Odette) in December 2021, causing around ₱20 billion in damages (Mendoza, 2021; Arquiza, 2022) with mangrove forests being heavily impacted due to their coastal location.

2. Data and Methods

2.1 Datasets

Data from the Sentinel-1 mission's dual-polarization C-band SAR device operating at 5.405GHz (C band) are provided, including ortho-corrected and calibrated S1 Ground Range Detected (GRD) scenes processed with the Sentinel-1 Toolbox. SAR polarizations such as VV, VH, VV+VH, VV/VH, were collected for pre-typhoon (December 1-15, 2021) and post-typhoon (December 16-31, 2021) periods, suitable for damage assessment and time-series analysis from 2021 to 2023, and CuSum analysis from November 2021 to December 2023.

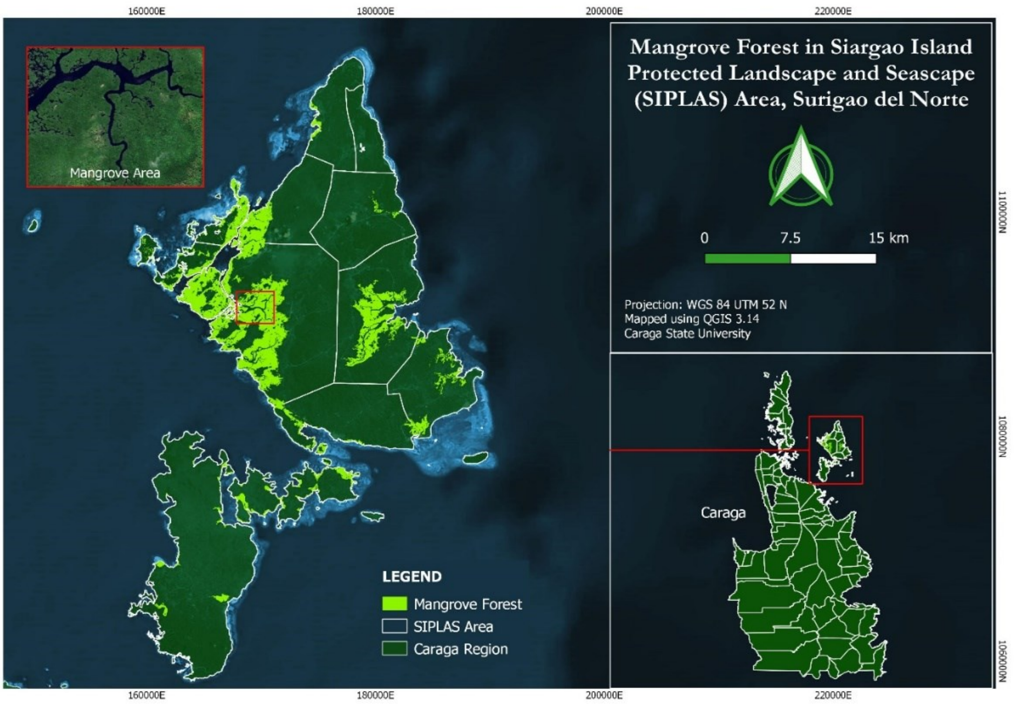

Figure 1. Map of Mangrove Forest Area in Siargao Island Protected Landscape and Seascape (SIPLAS), Siargao Island, Surigao del Norte.

2.2 Speckle Filtering

To reduce speckle noise, a smoothing filter with a specified radius of 50 meters was applied, improving visual clarity and interpretability of the images, particularly in areas with high noise levels or small-scale features.

2.3 Unsupervised SAR Log Ratio Change Detection in GEE

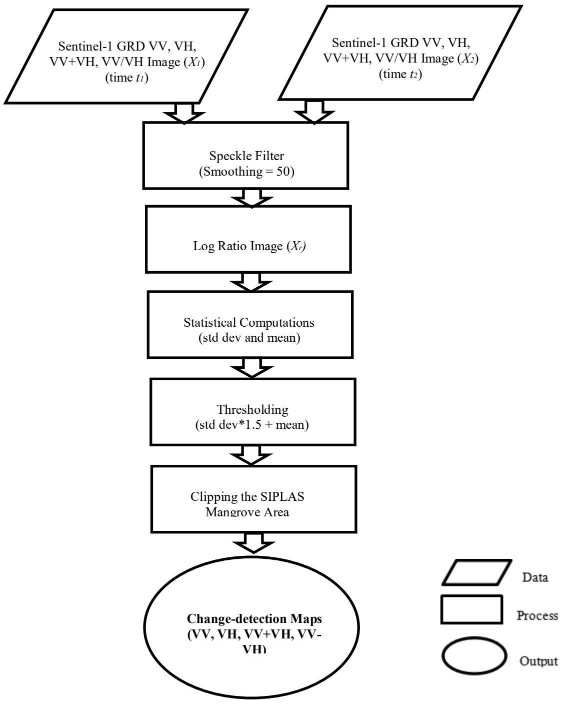

Figure 2. An overview of the Unsupervised SAR Change Detection process for Pre- and Post-Typhoon SAR Imagery in the Google Earth Engine (GEE) platform

2.3.1 Log Ratio Image Generation

Log-ratio images were generated through the subtraction of filtered SAR data from different time periods (pre- and post-typhoon images). This computational process facilitates the visualization and analysis of changes or differences in SAR signal intensities over time, aiding in identifying various phenomena such as land cover alterations or vegetation growth.

Log ratio operator is given by:

$$X_r = |log(\frac{X_2}{X_1})| = |log\,(X_2 - X_1)| \qquad (1)$$

2.3.2. Statistical Threshold for Change Classification

The mean and standard deviation values for each ratio image within the ROI at a 10-meter scale were calculated, and empirically derived thresholds ($1.5 * \text{std dev} + \text{mean}$) were used to identify areas with significant SAR signal changes. These thresholds were then applied to clip the ratio images and define mangrove regions using NAMRIA shapefiles in GEE.

2.4 Accuracy Assessment and Final Map Generation

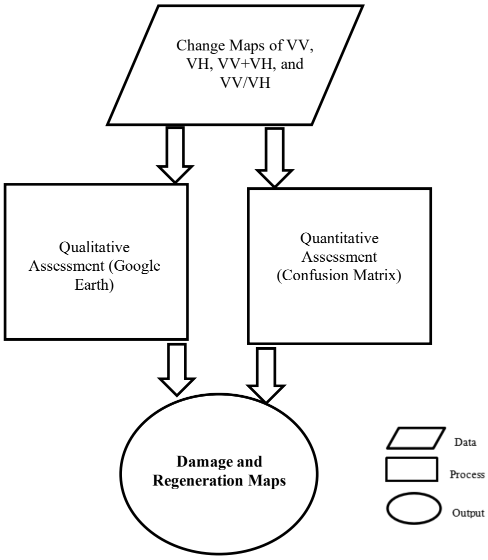

Figure 3. General Flowchart of Accuracy Assessment and Final Map Generation

2.4.1 Qualitative Assessment (Google Earth Image) and Quantitative Assessment (Confusion Matrix)

Google Earth Pro was used to download high-resolution post-typhoon images, examining change maps from four (4) polarization parameters. Also, the study employed a confusion matrix for evaluating classification models, aided by statistical thresholds derived from Intersection over Union (IoU) metrics, and assessed accuracy using 100 representative samples compared with a change detection map generated in Google Earth Engine (GEE). The key metrics were computed such as overall accuracy (OA, equation 2) , producer accuracy (PA, equation 3), user accuracy (UA, equation 4), and F-measure (F-score, equation 5) for each data cube using the confusion matrix. F-measure is particularly important as it balances the producer accuracy (PA) and overall accuracy (OA), prioritizing genuine detection over true negatives.

$$\textit{Overall Accuracy (OA)} = \frac{TP + TN}{(TP+TN+FP+FN)} \qquad (2)$$

$$\textit{Producer Accuracy (Recall)} = \frac{TP}{(TP+FN)} \qquad (3)$$

$$\textit{User Accuracy (Precision)} = \frac{TP}{(TP+FP)} \qquad (4)$$

$$\textit{F-measure} = \frac{2 * Recall * Precision}{(Recall + Precision)} \qquad (5)$$

where TP = True Positive, TN = True Negative, FP = False Positive, and FN = False Negative.

2.4.2 Final Map Generation (Damage and 2-year Time-Series Regeneration Maps)

The high-performing parameters were selected to create the damage extent map, using damage severity thresholds (Table 2) from Hoffman's study to classify damage levels. Regeneration maps were also generated based on these statistical thresholds.

Table 2. Definition of Damage Classes based on thresholds derived from Hoffman (2007).

Average Index Change	Damage Level Class
$X_r < 1.5$	No Damage
$1.5 \leq X_r < 2.0$	Light Damage
$2.0 \leq X_r < 2.5$	Significant Damage
$X_r \geq 2.5$	Severe Damage

2.5 Cumulative Sum (CuSum) Chart Generation in GEE

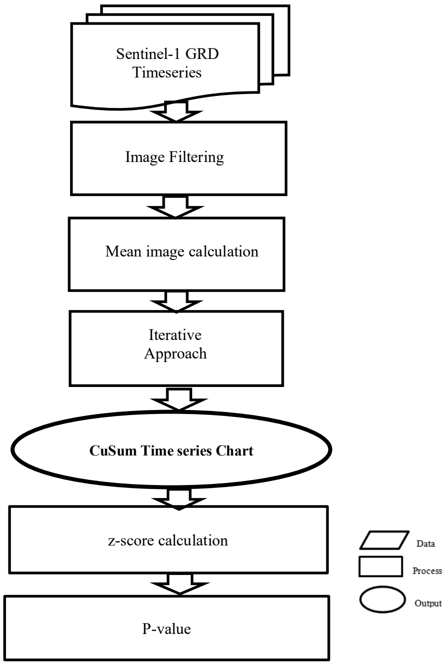

Figure 4. Flowchart in generating CuSum Chart in Google Earth Engine (GEE) and statistical calculation

2.5.1 Iterative Approach

The CuSum analysis was initiated by filtering the SAR Image Collection in Google Earth Engine (GEE) based on defined criteria such as the area of interest (AOI) and temporal range from November 1, 2021, to December 31, 2023. Subsequently, the Iterate Method was employed to calculate differences between the polarization images and their respective means, generating cumulative sum images representing CuSum values over time.

2.5.2 Z-Score and P-value calculation

The CuSum values, representing cumulative deviations from the process average, were analyzed to compute z-scores and p-values using Jasp, a statistical software. These calculations, performed within a 95% confidence interval, helped assess the statistical significance of observed deviations and supported the interpretation of CuSum values based on the null and alternative hypotheses.

3. Results and Discussion

3.1 Comparative Analysis of Pre- and Post-Typhoon Images of Different SAR Polarization Parameters in Detecting Changes Generated in GEE

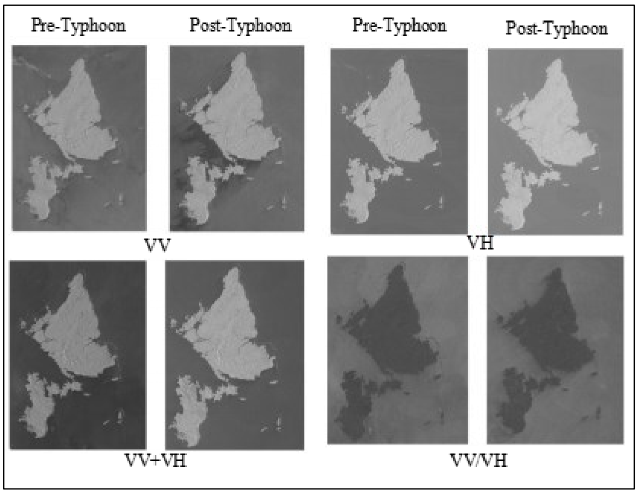

Figure 5. Pre-Typhoon and Post-Typhoon SAR Images in VV, VH, Combination of VV and VH, and VV/VH of SIPLAS generated in GEE.

The SAR images in Figure 5 generated in GEE depict the scenario of pre- and post-typhoons in the whole SIPLAS area. The pre-typhoon SAR image presents a baseline view of the SIPLAS area before the typhoon event, capturing the normal backscatter intensity distribution across different surface features. In contrast, the post-typhoon SAR image reflects alterations in backscatter intensity caused by the impact of the typhoon. Figure 5 provides a visual representation of these intensity changes, which present a change in this area. The pre-typhoon image exhibits a rough texture across various parts of the area, indicating high surface roughness and dense vegetation. In contrast, the post-typhoon image shows a smoother texture, suggesting changes in surface properties post-typhoon.

This is also revealed in the backscatter intensity and value of each of the polarization parameters (Figure 6). The proceeding figures reveal a notable shift in these values, with post-typhoon images displaying reduced backscatter counts. This indicates a discernible change in surface condition, indicative of damage occurring within the area under study.

Pre-typhoon VV counts range from -24 to -16.875, while post-typhoon VV counts extend from -30.25 to 6.25, indicating a shift in backscatter value distribution post-typhoon and suggesting alterations in surface characteristics affecting radar returns, particularly showing higher values post-typhoon, especially in negative bands, hinting at vegetation structure changes. In contrast, VH polarization demonstrates a marginal decline in counts post-typhoon. However, in comparison to VV polarization, the observed shift in trend is notably more substantial, owing to the pronounced decrease in count values across the same range of band values. Nevertheless, VH polarization exhibits a trend that closely aligns with the pre- and post-typhoon imagery, indicating limited variability in surface texture.

Among the polarization parameters examined, VV/VH showcases diverse intensity levels across bands, notably displaying elevated backscatter values in comparison to other polarization parameters. Nonetheless, akin to other parameters, there is an abrupt transition in backscatter counts, leading to fluctuation as intensity increases.

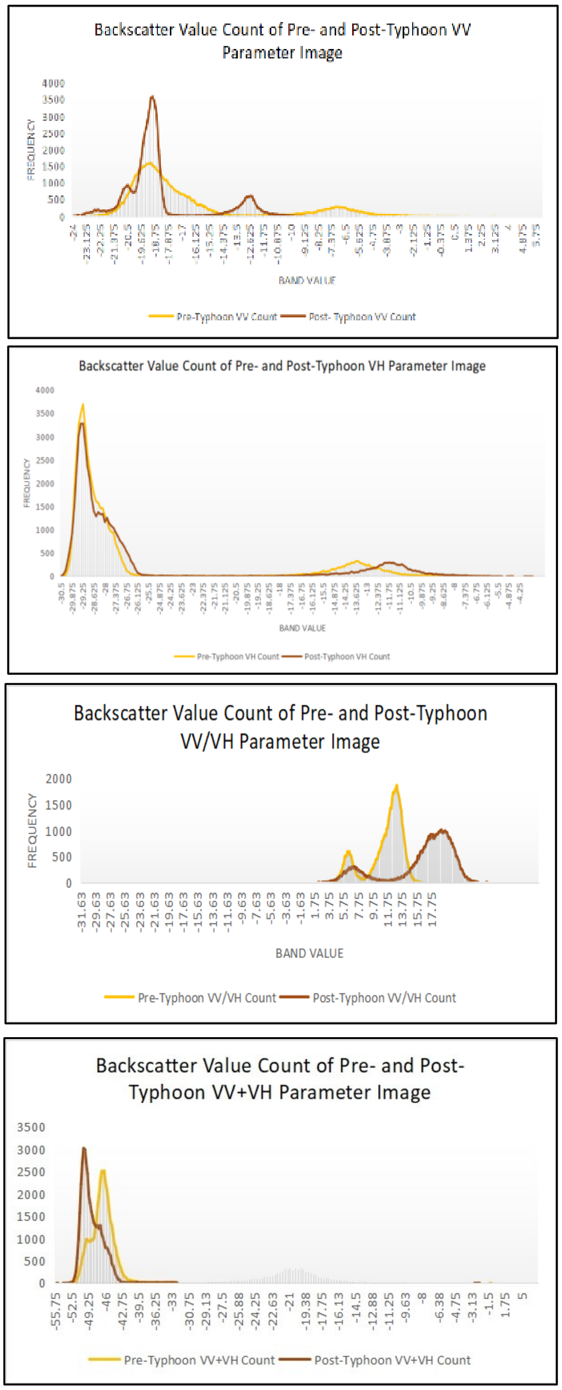

Figure 6. Comparison of backscatter values of Pre-typhoon and Post-Typhoon SAR images from different

3.2 Log Ratio Images and Mangrove Change Map

The data in Figure 7 demonstrates the effectiveness of different polarization parameters in detecting damage through log ratio values. VV polarization shows higher variability (mean = 1.562, SD = 1.181) compared to VH polarization (mean = 0.937, SD = 1.139), indicating VV's superior damage detection capacity. The combined VV and VH mean (1.709, SD = 1.819) and the VV/VH mean ratio (0.721, SD = 1.154) suggest an overall increase in backscatter intensity post-event, with these parameters providing extensive coverage for detecting damage, which illustrate significant shifts in backscatter characteristics post-event.

Of particular interest in this study is the delineation of the mangrove area in SIPLAS, where the variability of change across each polarization parameter is evident (Figure 8). The combined VV and VH values delineate more pronounced areas damage vegetation mask compared to VV or VH individually. Notably, VV exhibits a more discernible change compared to other parameters.

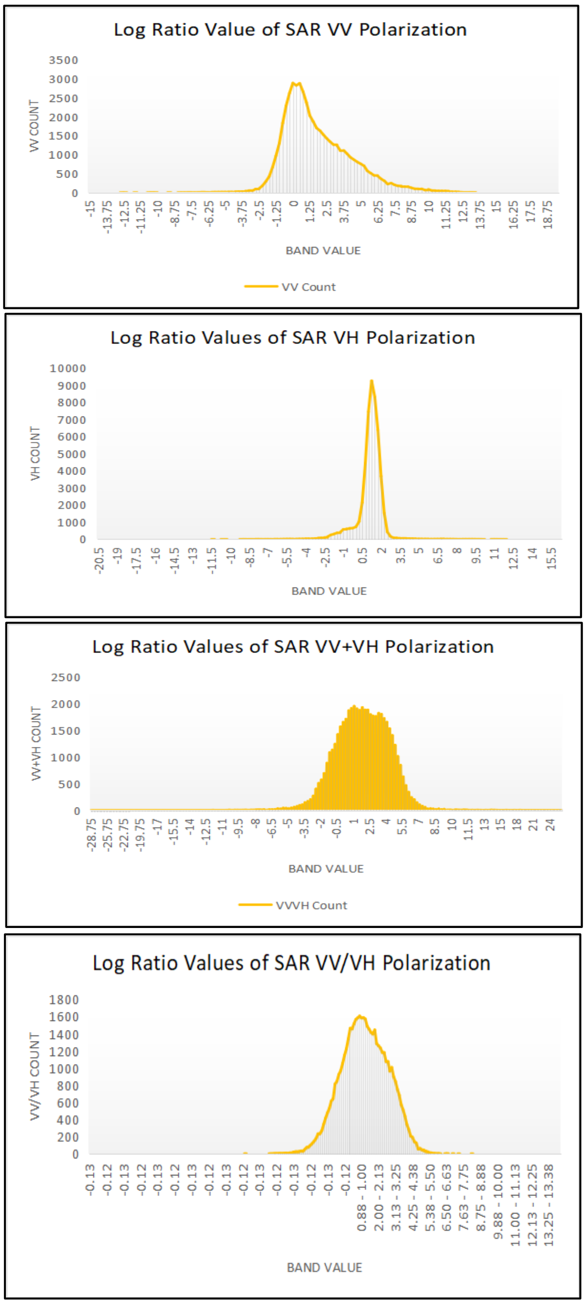

Figure 7. Comparison of log ratio values of SAR Polarization Parameter (VV,VH.VV+VH,VV/VH)

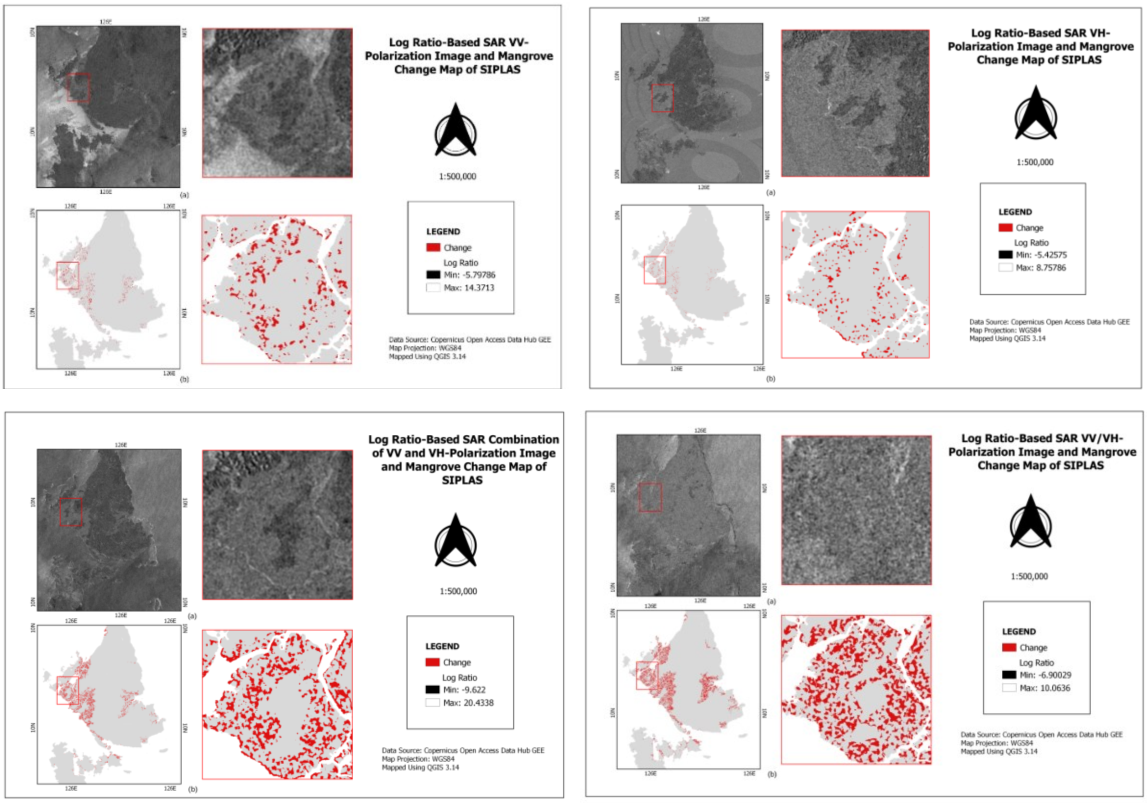

Figure 8. Comparison of log ratio value and Change Map of the four Polarization Parameters for Pre- and Post-Typhoon Images

3.3 Quantitative and Qualitative Accuracy Assessment of Mangrove Change Map

In this study, two methods were employed to assess the accuracy of the unsupervised method for change detection. The qualitative assessment conducted alongside the quantitative analysis plays a significant role in validating the efficacy of SAR polarization parameters for detecting mangrove damage. This validation process utilized visual representations through Google Earth Pro, enhancing the credibility of the results.

3.3.1 Qualitative Assessment of Mangrove Change Map

The illustration in Figure 9 presents a comparative assessment of different polarization parameters in effectively discerning damage. The reference image, derived from Google Earth on December 19, 2021, following the typhoon, visually delineates the extent of the typhoon's impact on mangrove areas, identifiable through brown coloration indicating damage.

Each polarization parameter exhibits varying levels of detected damage; however, VV polarization showcases the most promising outcomes by encompassing a larger portion of the affected area. In contrast, some damages were not directly identified, and certain areas were misclassified, as depicted in the reference image. For instance, the combined VV and VH, as well as the VV/VH ratio parameters, generalized the extent of damage.

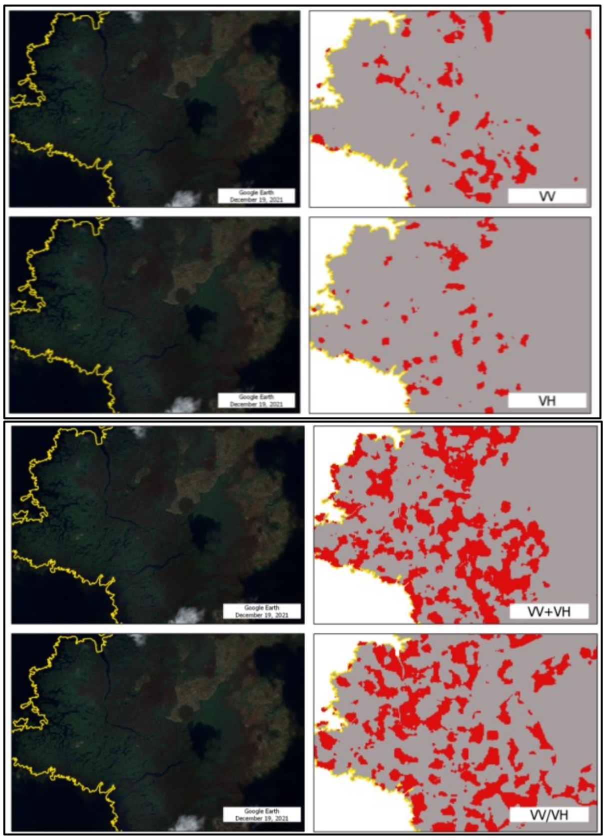

Figure 9. Comparison of different polarization parameters (on the right side) for damage detection in google earth with the reference image (on the left side)

3.3.2 Quantitative Assessment of Mangrove Change Map

The confusion matrix for the VV polarization parameter (Table 2) reveals its high accuracy in detecting significant damage, with a producer's accuracy of 0.89 for damaged pixels and an overall accuracy (OA) and F-measure of 0.92. This accuracy is visually supported by the alignment of identified damaged areas with brown regions in the post-typhoon image. Conversely, the VH polarization parameter shows slightly lower accuracy, with a producer's accuracy of 0.87 and an OA and F-measure of 0.875, indicating slightly less effectiveness compared to VV. The combined VV and VH polarization parameters and the VV/VH ratio parameter also show strong but slightly lower accuracy metrics compared to VV alone, suggesting that the combination does not significantly enhance damage detection. Overall, VV polarization is the most promising parameter for identifying mangrove damage in SIPLAS, corroborated by similar findings in a study by Ygorra et al. (2021).

Table 2. Accuracy Assessment of the four (4) polarization parameters

	VV	VH	VV+VH	VV/VH
User’s Accuracy	95%	88%	76%	76%
Producer’s Accuracy	89%	87%	90%	89%
Overall Accuracy	92%	87.5%	80.5%	80.5%
F-measure	0.92	0.87	0.82	0.82

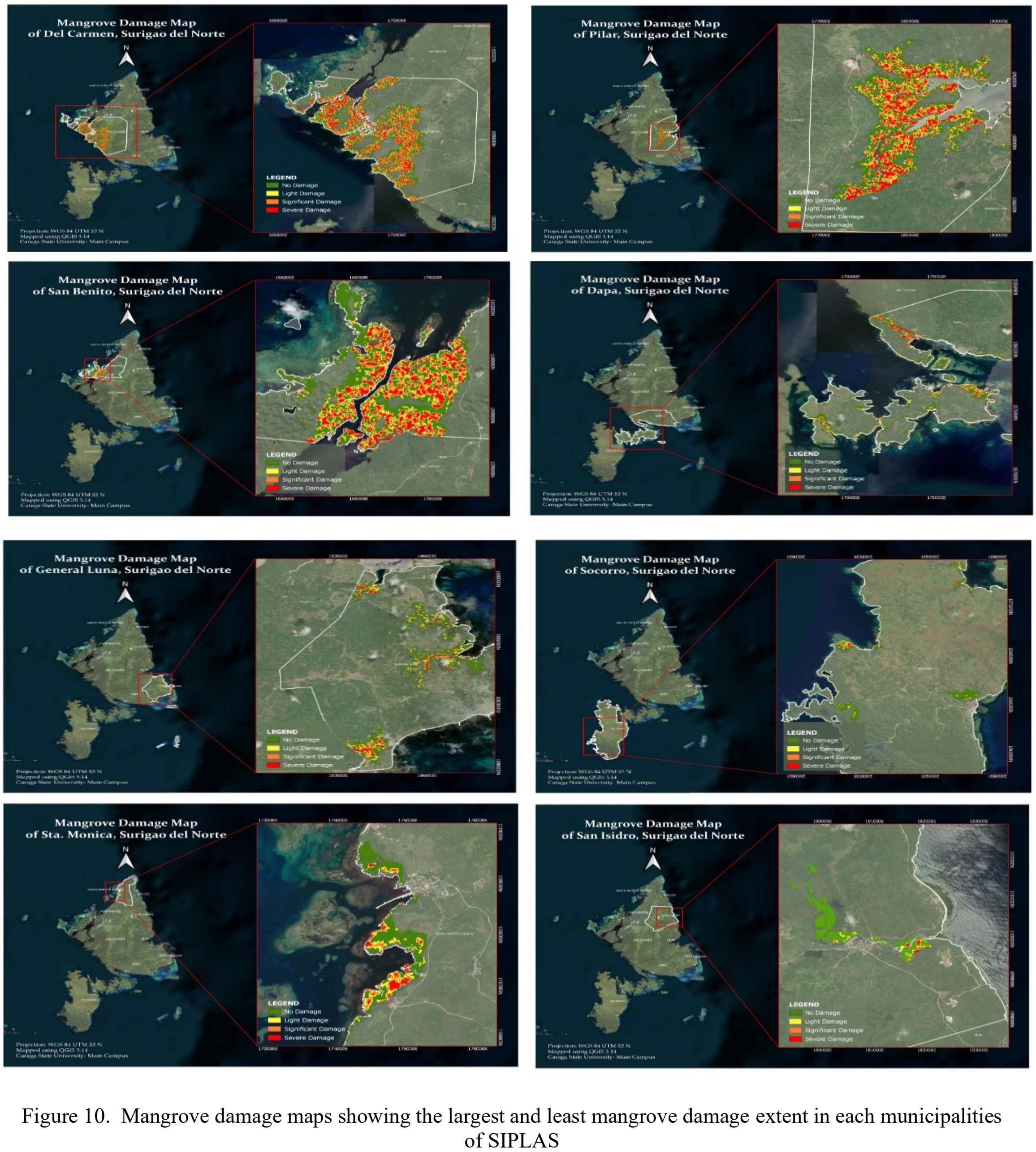

Figure 10. Mangrove damage maps showing the largest and least mangrove damage extent in each municipalities of SIPLAS

3.4 Mangrove Damage Assessment in SIPLAS

SIPLAS covers nine (9) municipalities of Surigao del Norte located in Siargao Island: Burgos, Dapa, Del Carmen, General Luna, Pilar, San Benito, San Isidro, Santa Monica, and Socorro. Among these municipalities, Del Carmen has the largest coverage of mangrove forest (Figure 10).

The Mangrove Damage Map of Dapa, Surigao del Norte, shows that out of 685.88 hectares, 424.89 hectares remain undamaged, 105.82 hectares have light damage, 73.55 hectares have significant damage, and 81.62 hectares have severe damage, with the most severe damage concentrated along coastlines and river mouths. Similarly, in Del Carmen, out of 4879.68 hectares, 2185.91 hectares are unaffected, 861.71 hectares have light damage, 808.38 hectares have significant damage, and 1023.68 hectares have severe damage, with the most severe damage along the coast and riverbanks. General Luna has 253.84 hectares undamaged, 60.89 hectares lightly damaged, 40.43 hectares significantly damaged, and 35.51 hectares severely damaged, with severe damage concentrated in southern tips and eastern inlets.

In Pilar, 580.83 hectares remain undamaged, 272.66 hectares have light damage, 250.08 hectares have significant damage, and 291.59 hectares have severe damage, mainly along waterways and southern coastline. San Benito has 510.63 hectares undamaged, 215.61 hectares lightly damaged, 200.41 hectares significantly damaged, and 217.54 hectares severely damaged. San Isidro has 55.69 hectares undamaged, 4.98 hectares lightly damaged, 2.18 hectares significantly damaged, and 1.57 hectares severely damaged. Socorro shows 178.84 hectares undamaged, 27.77 hectares lightly damaged, 15.3 hectares significantly damaged, and 13.35 hectares severely damaged, with severe damage closer to the coastline. Sta. Monica has 57.13 hectares undamaged, 14.04 hectares lightly damaged, 10.23 hectares significantly damaged, and 6.21 hectares severely damaged, with severe damage in the most exposed areas.

Table 3 and Figure 11 details the extent of mangrove damage across nine municipalities in the Siargao Island Protected Landscape and Seascape (SIPLAS), categorizing the damage as no damage, light damage, significant damage, and severe damage. The data reveals that 4247.76 hectares of mangroves are undamaged, 1563.48 hectares have light damage, 1400.56 hectares have significant damage, and 1671.07 hectares have severe damage, indicating varying degrees of mangrove disturbance across SIPLAS. Figure 25 shows San Isidro has the highest percentage of undamaged mangroves at 86.45%, while Pilar has the lowest at 41.63%. Del Carmen has the highest percentage of severely damaged mangroves at 20.98%, followed closely by Pilar at 20.90%, with overall damage affecting 53% of the total mangrove forest area in SIPLAS.

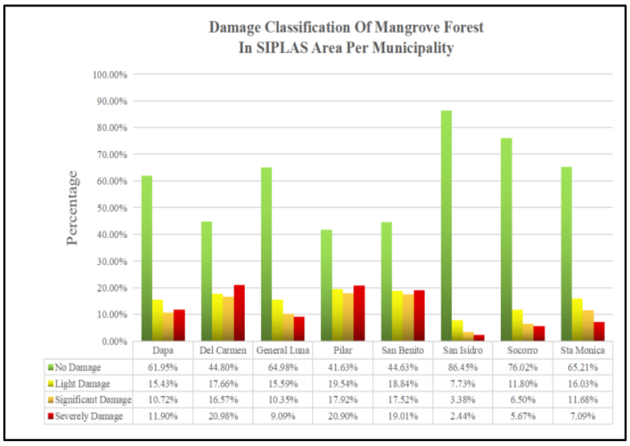

Figure 11. Rate of mangrove damage in the Municipalities under Siargao Island Protected Landscape and Seascape (SIPLAS) area based on Hoffman’s Classification.

Table 3. Post-disaster classification of damage in the Municipalities under Siargao Island Protected Landscape and Seascape (SIPLAS) area based on Hoffman’s Classification

Municipality	CLASS				Total (ha)
	No Damage (ha)	Light Damage (ha)	Significant Damage (ha)	Severe Damage (ha)	
Dapa	424.89	105.82	73.55	81.62	**685.88**
Del Carmen	2185.91	861.71	808.38	1023.68	**4879.68**
General Luna	253.84	60.89	40.43	35.51	**390.67**
Pilar	580.83	272.66	250.08	291.59	**1395.16**
San Benito	510.63	215.61	200.41	217.54	**1144.19**
San Isidro	55.69	4.98	2.18	1.57	**64.42**
Socorro	178.84	27.77	15.3	13.35	**235.26**
Sta Monica	57.13	14.04	10.23	6.21	**87.61**
Total	**4247.76**	**1563.48**	**1400.56**	**1671.07**	**8882.87**

3.5 Mangrove Regeneration Dynamics

To assess the trend of regeneration, the study utilized two distinct methodologies. First, it employed the log ratio of time-series SAR images, examining changes over time to identify signs of regeneration initiation. Additionally, CuSum analysis was applied to estimate the specific timeframe when the regeneration process commenced.

3.5.1 Time-Series Regeneration Maps of SIPLAS

To visualize the regeneration dynamics after assessing the extent of mangrove damage in SIPLAS area, a time series regeneration maps and a quantitative analysis were made. A quantitative analysis was employed to provide a numerical view of regeneration by quantifying the recovery in terms of its rate of regeneration over time.

Table 4. Regeneration of mangrove forest in hectares in each municipality from 2022 and 2023.

Municipality	Regeneration 2022 (ha)	Regeneration 2023 (ha)
Dapa	81.14	162.91
Del Carmen	924.66	1543.08
General Luna	62.49	85.97
Pilar	439.37	475.18
San Benito	220.13	325.47
San Isidro	5.49	7.41
Socorro	18.87	30.51
Sta. Monica	11.44	29.62
Total	**1763.59**	**2660.15**

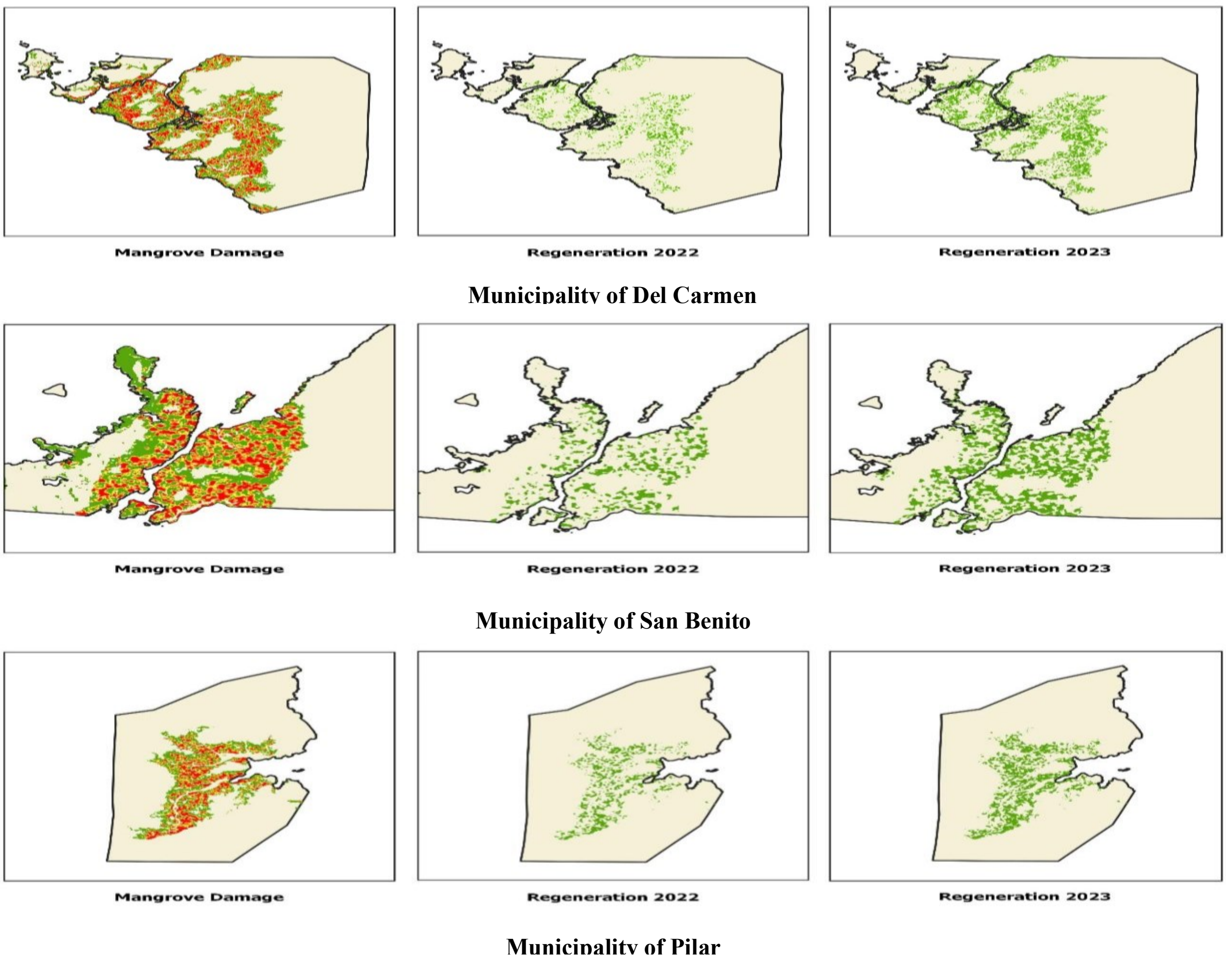

Figure 12. Regeneration maps of the municipalities with the largest extent of mangrove forests in SIPLAS area

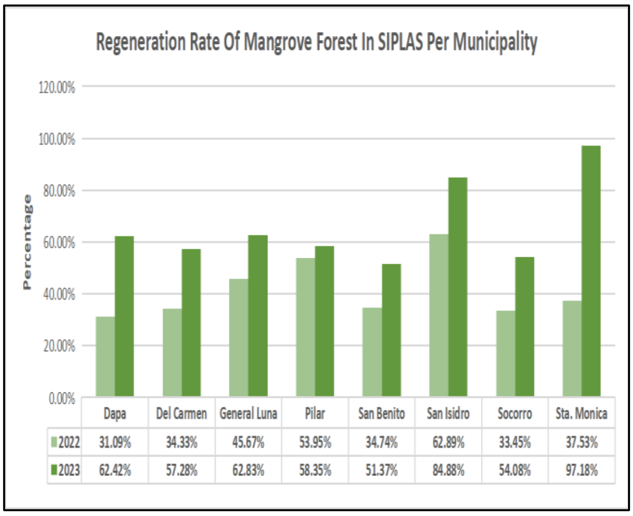

Figure 13. Regeneration rate of Mangrove Forest in SIPLAS per Municipality.

3.5.2 Cumulative Sum (CuSum) Analysis

Cumulative Sum (CuSum) analysis has predominantly found application within the financial sector for assessing alterations within their defined objectives. Moreover, its utility extends to the monitoring of vegetative and structural damage due to its sensitivity to change. In this study, this analytical approach was specifically leveraged to ascertain the regeneration dynamics of mangrove ecosystems following a typhoon event.

Figure 14 provides a graphical representation of the cumulative sum trend relative to the mean values of VV polarization. This visualization offers insight into the evolving variability within the time-series dataset.

The analysis of this data, conducted with a 95% confidence level, yielded p-values derived from calculated z-scores. One such critical point occurs on September 16, 2022, where a substantial decrease in CuSum from -0.844 to -0.896 is observed, accompanied by a decrease in the corresponding z-score from -1.571 to -1.747. This shift is further supported by a low p-value of 0.040, indicating statistical significance and rejecting the null hypothesis of ‘no change’. This is also evident from the interview conducted, in which one of the respondents asserted that the start of the sign of regeneration took almost a year.
Similarly, on October 22, 2022, another significant shift is noted with a decrease in CuSum from -0.825 to -0.862, a decrease in z-score from -1.507 to -1.632, and a low p-value of 0.051. These dates signify periods of potential active regeneration or recovery within the mangrove ecosystem, as indicated by these CuSum values. Additionally, the shift points on September 4, 2022, and January 14, 2023, further reinforce these findings, highlighting the sensitivity of CuSum analysis in detecting changes in vegetation post-disturbance.

4. Conclusion

Mangroves are crucial to coastal ecosystems, providing biodiversity hotspots and protection against natural disasters like typhoons, floods, and storm surges. In the Philippines, which faces about 20 typhoons annually, Super Typhoon Rai in 2021 severely damaged the mangrove forests on Siargao Island. Monitoring their recovery is vital for effective conservation and sustainable development. Traditional satellite imagery faces limitations like cloud cover, so this study uses Synthetic Aperture Radar (SAR) data, which penetrates clouds, to track forest damage and regeneration over time in the Siargao Island Protected Landscapes and Seascape (SIPLAS) area via Google Earth Engine (GEE).

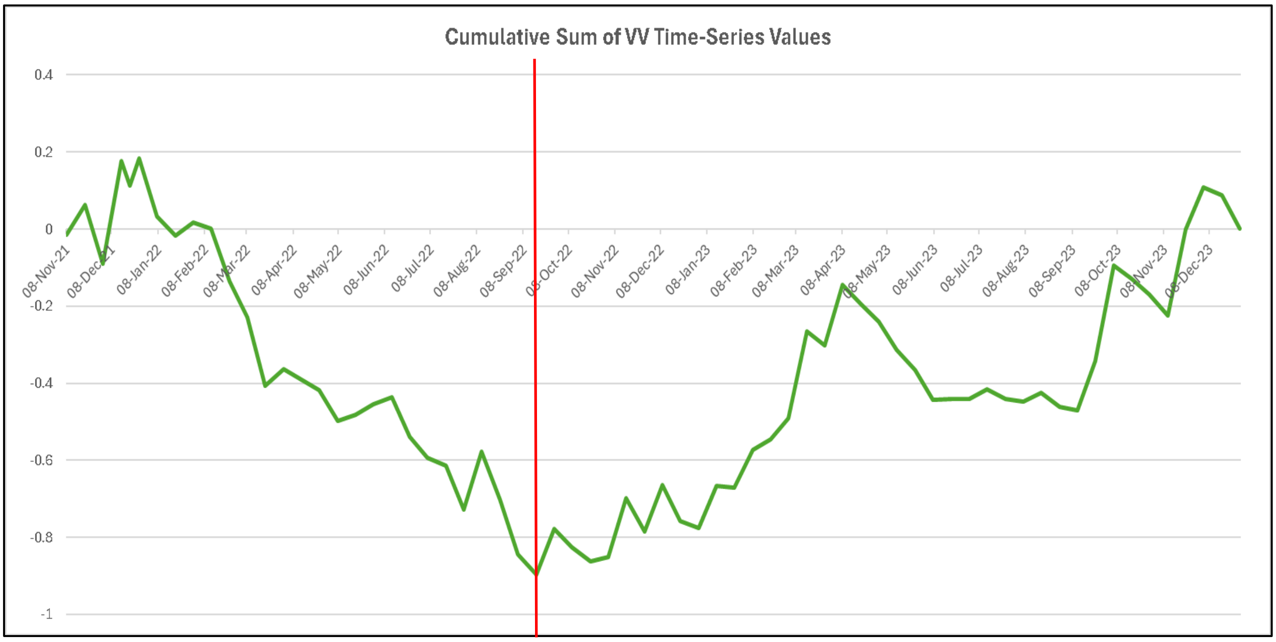

Figure 14. Cumulative Sum (CuSum) of VV Polarization values from November 2021 to December 2023 generated in GEE

The research focuses on assessing SAR polarization to detect changes, mapping typhoon damage, and analyzing mangrove regeneration dynamics using time-series and Cumulative Sum (CuSum) analysis.

After employing the methods and procedures in assessing the post-disaster recovery of mangrove forests in SIPLAS area, the results showed that among the SAR polarization parameters, VV polarization yielded a promising overall accuracy of 92% and an F-measure of 0.92. Conversely, the VH polarization showed an overall accuracy of 87.5% and an F-measure of 0.87. Meanwhile, the combination of VV and VH, and VV/VH achieved an overall accuracy of 80.5% with an F-measure of 0.82. Additionally, the study found that 53% of the mangrove forests in the SIPLAS area were damaged. Detailed analysis of the damage across municipalities showed varying extents of mangrove damage with Dapa of up to 260.99 ha, Del Carmen 2,693.77 ha, General Luna 136.83 ha, Pilar 814.33 ha, San Benito 633.56 ha, San Isidro 8.73 ha, Socorro 56.42 ha, and Sta. Monica 30.48 ha.

Following the assessment of mangrove damage in the SIPLAS area, the regeneration dynamics within the area were evaluated for 2022 and 2023. The regeneration rates differed across different municipalities. Dapa showed a regeneration rate of 31.09% in 2022 and increased to 62.42% in 2023. Del Carmen regenerated at 34.33% in 2022 and 57.28% in 2023, while General Luna showed a higher rate of 45.67% in 2022 and 62.83% in 2023. Pilar, San Benito, San Isidro, Socorro, and Sta. Monica also demonstrated significant regeneration progress over the two years. Notably, Sta. Monica had the highest increase, from 37.53% in 2022 to 97.18% in 2023. To sum up, the mangrove forest in SIPLAS area has a regeneration rate of up to 38.09% in 2022 and 57.35% in 2023, respectively.

After evaluating the regeneration dynamics, a Cumulative Sum (CuSum) analysis was used to monitor the regeneration and it shows significant shifts indicating potential active regeneration or recovery within the mangrove ecosystem. On September 16, 2022, a substantial decrease in CuSum along with a decrease in z-score and a low p-value (0.040) signify statistical significance. Similarly, on October 22, 2022, another notable shift is observed. Additional shift points on September 4, 2022, and January 14, 2023, further support these findings, highlighting the sensitivity of CuSum analysis in detecting post-disturbance vegetation changes. Ultimately, the trend across the SIPLAS area shows a dynamic and progressive recovery over time.

5. Recommendation

This study demonstrates that using Sentinel-1 SAR imagery for damage assessment mapping produces invaluable outcomes through the application of an unsupervised log ratio change detection method and regeneration assessment employing time-series and CuSum analysis in Google Earth Engine. Employing this method enhances the capability to detect changes accurately, particularly when using the correct polarization parameters. However, further enhancements and more substantial results can be achieved by:

i. Investigate a wider range of polarization parameters from other SAR Data beyond VV and VH, to determine the most suitable parameters for detecting damage and assessing other factors impacting mangrove health.
ii. Integrate optical imagery, such as multispectral or hyperspectral data, alongside SAR data to complement and support damage assessment and regeneration monitoring.
iii. Expand the use of Cumulative Sum (CuSum) analysis to encompass a more comprehensive range of variables and temporal aspects. This includes exploring different thresholds, time intervals, and statistical metrics within the CuSum framework to effectively capture and quantify changes in mangrove conditions over time. Additionally, consider integrating CuSum analysis with other change detection algorithms or machine learning techniques to further refine the assessment of mangrove damage and regeneration dynamics.

References

Arquiza, Y. (2022, October 3). *Siargao islanders rebuild lives after Typhoon Odette*. SunStar Publishing Inc. https://www.sunstar.com.ph/davao/feature/siargao-islanders-rebuild-lives-after-typhoon-odette

Earth Science Data Systems, N. (2024, May 7). *Synthetic Aperture Radar (SAR) | Earthdata*. Www.earthdata.nasa.gov. https://www.earthdata.nasa.gov/technology/synthetic-aperture-radar-sar#:~:text=Synthetic%20aperture%20radar%2C%20or%20SAR%2C%20uses%20the%20microwave

Encyclopedia Britannica. (2019). mangrove | Definition, Types, Importance, Uses, & Facts. In *Encyclopædia Britannica*. https://www.britannica.com/plant/mangrove

Hoffmann, J. (2007). Mapping damage during the Bam (Iran) earthquake using interferometric coherence. *International Journal of Remote Sensing*, *28*(6), 1199–1216. https://doi.org/10.1080/01431160600928567

Mendoza, J. E. (2021, December 17). *LOOK: Typhoon Odette leaves Siargao Island ravaged*. INQUIRER.net. https://newsinfo.inquirer.net/1529010/look-typhoon-odette-leaves-siargao-island-ravaged

Molthan, A., Bell, J., & Schultz, L. (2017). *Advantages and Applications of Synthetic Aperture Radar as a Decision Support Tool*. https://ntrs.nasa.gov/api/citations/20170011226/downloads/20170011226.pdf

NASA. (2020, May 12). *ARSET - Forest Mapping and Monitoring with SAR Data | NASA Applied Sciences*. Appliedsciences.nasa.gov. https://appliedsciences.nasa.gov/get-involved/training/english/arset-forest-mapping-and-monitoring-sar-data#:~:text=Radar%20remote%20sensing%20overcomes%20these%20challenges%20because%20of

NASA Applied Sciences. (2021, December 16). *Super Typhoon Rai (Odette) 2021 | NASA Applied Sciences*. Appliedsciences.nasa.gov. https://appliedsciences.nasa.gov/what-we-do/disasters/disasters-activations/super-typhoon-rai-odette-2021

Philippine News Agency. (2022). *About the Agency | Philippine News Agency*. www.pna.gov.ph. https://www.pna.gov.ph/about

One News Ph. (2017). *Some Siargao Residents Saved By Mangrove Forest From Odette | OneNews.PH*. Some Siargao

Residents Saved by Mangrove Forest from Odette | OneNews.PH. https://www.onenews.ph/articles/some-siargao-residents-saved-by-mangrove-forest-from-odette

Santos, G. D. C. (2021). 2020 tropical cyclones in the Philippines: A review. *Tropical Cyclone Research and Review*, *10*(3), 191–199. https://doi.org/10.1016/j.tcrr.2021.09.003

SIPLAS. (2013). *SIPLAS | Siargao Island Protected Landscape and Seascape (Philippines)*. Siplas.org. http://siplas.org/

Stringer, L. C., & Orchard, S. (2013). *Mangroves, nature's shield against typhoons and tsunami*. The Conversation. https://theconversation.com/mangroves-natures-shield-against-typhoons-and-tsunami-21051

The Nature Conservancy. (2021, July 26). *State of the World's Mangroves*. The Nature Conservancy. https://www.nature.org/en-us/what-we-do/our-insights/perspectives/state-of-world-mangroves/

The Philippines Today. (2021, April 28). *Siargao Islands Protected Landscape And Seascape* . https://thephilippinestoday.com/siargao-islands-protected-landscape-and-seascape/

Urban Nature Atlas. (2022). *Siargao It Up: Mangrove Conservation | Urban Nature Atlas*. Una.city. https://una.city/nbs/del-carmen/siargao-it-mangrove-conservation

Villamente, J. (2023, February 23). *Siargao mangrove reserve gets recognition. Daily Tribune*. Tribune. https://tribune.net.ph/2023/02/24/siargao-mangrove-reserve-gets-recognition

Visit Del Carmen. (2024). *Largest Contiguous Mangrove Forest in the Philippines*. Municipality of Del Carmen. https://www.visitdelcarmen.com/largest-contiguous-mangrove-forest-in-the-philippines/

Viray-Mendoza, V. (2017, November 22). *Mangrove Forests in the Philippines – The Maritime Review*. Maritimereview.ph. https://maritimereview.ph/mangrove-forests-in-the-philippines/

Ygorra, B., Frappart, F., Wigneron, J. P., Moisy, C., Catry, T., Baup, F., Hamunyela, E., & Riazanoff, S. (2021). Monitoring loss of tropical forest cover from Sentinel-1 time-series: A CuSum-based approach. *International Journal of Applied Earth Observation and Geoinformation*, *103*, 102532.